

Article

Reliability Analysis of Concrete Gravity Dams Based on Least Squares Support Vector Machines with an Improved Particle Swarm Optimization Algorithm

Shida Wang, Bo Xu * , Zhenhao Zhu, Jing Li and Junyi Lu

College of Hydraulic Science and Engineering, Yangzhou University, Yangzhou 225009, China

* Correspondence: xubo@yzu.edu.cn

Abstract: A reliability analysis method based on least squares support vector machines with an improved particle swarm optimization algorithm (IPSO-LSSVM) is proposed to calculate the reliability of concrete gravity dams when explicit nonlinear limit-state functions are difficult to obtain accurately. First, the main failure modes of concrete gravity dams and their influencing factors are determined. Second, Latin hypercube sampling is used to create samples. A finite element calculation batch program of concrete gravity dams is written to calculate the safety indexes of each sample. Third, based on the samples, the IPSO-LSSVM model is established to replace the finite element calculation. Finally, the failure probability of concrete gravity dams is obtained by using the Monte Carlo (MC) method. The case study for a typical concrete gravity dam in the Yunnan Province of China shows that the dam is reliable because the failure probability is 8.87×10^{-5} . The proposed reliability analysis method is efficient and feasible for calculating the reliability of concrete gravity dams.



Citation: Wang, S.; Xu, B.; Zhu, Z.; Li, J.; Lu, J. Reliability Analysis of Concrete Gravity Dams Based on Least Squares Support Vector Machines with an Improved Particle Swarm Optimization Algorithm.

Appl. Sci. **2022**, *12*, 12315.
<https://doi.org/10.3390/app122312315>

Academic Editors: Tongchun Li and Chaoning Lin

Received: 25 October 2022
Accepted: 30 November 2022
Published: 1 December 2022

Publisher's Note: MDPI stays neutral with regard to jurisdictional claims in published maps and institutional affiliations.



Copyright: © 2022 by the authors. Licensee MDPI, Basel, Switzerland. This article is an open access article distributed under the terms and conditions of the Creative Commons Attribution (CC BY) license (<https://creativecommons.org/licenses/by/4.0/>).

Keywords: concrete gravity dam; reliability analysis method; improved particle swarm optimization algorithm; least squares support vector machine; Monte Carlo method

1. Introduction

Concrete gravity dams are a very common type of dam built and used in China, and the total construction volume is among the highest in the world. Ensuring that concrete gravity dams can meet reliability requirements throughout the operation period is of great significance to national security construction and ecological environmental protection. The single safety factor method is mostly used in the design of concrete gravity dams with a long operation stage. The variables affecting the dam structure design, such as material properties and external loads, are random variables, not certain values. The safety factor method only uses a certain safety factor to evaluate the safety of the dam, without considering the objective uncertainty in each design variable. The reliability analysis for the design and safety check of concrete gravity dams can effectively overcome the shortcomings of the safety factor method [1,2]. The results obtained by reliability analysis are more reliable.

The traditional reliability analysis methods mainly include the first-order reliability method [3], MC method [4], response surface method [5], and direct integration method [6]. However, all of these methods have certain shortcomings. For example, the accuracy of the first-order reliability method is not high; the MC method requires a large number of finite element calculations to obtain the results with high accuracy, and the computational cost is relatively large; the response surface method is generally polynomial in form, which, to a certain extent, limits the accuracy of its fitted limit state function, and the calculation will be more complicated when dealing with a high degree of nonlinearity and a large number of variables; and the direct integration method often generates computational difficulties.

To overcome the limitations of the application of the above-mentioned traditional reliability analysis methods, many scholars have conducted useful research. Zhao et al. [7] proposed the third-order moment method based on the study of the primary second-order moment method, which improved the accuracy of the reliability calculation results. Lu et al. [8] proposed a second fourth-order moment calculation method for reliability calculations based on the first fourth-order moment of the second-order approximation of the functional function and proved its simplicity and accuracy. Jiang et al. [9] proposed a reliability analysis method for gravity dams based on the Hermite orthogonal polynomial approximation method and illustrated the correctness and effectiveness of the proposed method by arithmetic examples. Ren et al. [10] proposed a sensitivity-assisted MC simulation method in which second-order derivatives were introduced to improve the accuracy of reliability calculations. Heydt et al. [11] proposed a bootstrap-compensated MC method to reduce the computation time of reliability by introducing the concept of augmented samples. The importance sampling method [12] is an improved MC method, which is mainly used to improve the efficiency of simulation calculations. Guan et al. [13] discussed that a change in the location of the implicit functional function fitting point in the traditional response surface method can affect the results of structural reliability calculations, indicating that the accuracy of response surface method calculations at the checkpoint is closely related to the location of the checkpoint. Zhu et al. [14] proposed a weighted dynamic response surface reliability analysis method based on the cat swarm algorithm, which overcomes the drawback of the MC method that requires a large number of repeated samples. Zhao [15] proposed a reliability solution method for the response surface of a high-dimensional model combined with the first-order reliability method to solve the structural reliability. Balu et al. [16] proposed a new method for solving implicit functional function reliability problems, which does not require the derivation of response surface functions of random variables in the process of calculating reliability. Sundar et al. [17] used locally propagated samples to track the response surface function, and an important feature of this algorithm is that the alternative model advances with the choice of samples, enabling the algorithm to converge quickly to the response surface. Yuan et al. [18] proposed an improved method of conditional boundary integration method for solving reliability problems with high accuracy requirements by using the direct integration method, which adopts a simple modification of binary integration based on the probability addition rule, and the computational accuracy and efficiency of the method were verified by the error analysis of arithmetic cases. Although scholars have improved and proposed many new methods to address the shortcomings of the traditional reliability solution methods, the following shortcomings still exist: the applicability and solution accuracy of some reliability calculation methods are limited due to the complexity of actual structural engineering problems and the existence of highly nonlinear failure surfaces.

The limit state functions of concrete gravity dams are often highly nonlinear when considering the randomness of external loads, material parameters, and other factors. Therefore, it is difficult to express them accurately with explicit functions. When solving such problems using the above reliability solution methods, it is usually difficult to ensure the accuracy and efficiency of the calculation results.

The development of machine learning and intelligent algorithms provides effective tools for solving practical engineering problems, especially in solving engineering reliability problems [19,20]. Least squares support vector machine (LSSVM) is a new generation of machine learning method. LSSVM has advantages of rigorous mathematical foundation, strong small-sample learning ability, low over-fitting risk, fast solving speed, etc. However, in practical application, it is difficult to determine hyper-parameters of LSSVM. For example, when the radial basis function is adopted as kernel function, it is hard to determine its penalty parameter γ and kernel width parameter σ . At present, optimizing the search algorithm is the main approach to solving the above problem. The particle swarm optimization (PSO) algorithm [21] is widely used to tune the hyper-parameters of the LSSVM because of its simple form and easy understanding [22–25]. However, the PSO algorithm

has the drawback of easily falling into the local optimum, so this paper improves the PSO algorithm for the hyper-parameters tuning.

To improve the calculation accuracy and efficiency, this paper proposed a reliability analysis method based on least squares support vector machines with an improved particle swarm optimization algorithm (IPSO-LSSVM). The IPSO-LSSVM is adopted to establish the response surface to approximate the limit state function based on the samples generated by computer experiments. Subsequently, the proposed response surface is utilized in conjunction with the Monte Carlo (MC) method to obtain the desired reliability estimation.

2. Methodology

2.1. Reliability Analysis of Concrete Gravity Dams

For concrete gravity dams, the main failure modes include sliding instability along the dam–ground surface and overstress of the dam heel and dam toe. Each of these three failure modes needs to be mathematically described by a limit-state function to conduct reliability analysis and calculate the failure probability (P_f) for concrete gravity dams.

Sliding along the dam–ground surface is the first failure mode taken into consideration. The dam will slide if the horizontal hydrostatic pressure exceeds the sliding shear strength. This failure mode's limit-state function is expressed as follows:

$$Z_1 = K_c - 1 \quad (1)$$

where K_c is the anti-sliding stability safety factor along the dam–ground surface.

When the finite element method is used, the limit-state function can also be expressed as:

$$Z_1 = \sum_{i=1}^d (-f'\sigma_{yi} + c' - \tau_{xyi})b_i \quad (2)$$

where d is the total number of elements of the dam–ground surface; f' is the anti-shear friction coefficient; c' is the anti-shear cohesion; b_i is the edge length of element i along the sliding surface; and σ_{yi} , τ_{xyi} are the vertical normal stress and shear stress of element i , respectively.

The other two failure modes considered are the overstress of the dam heel and toe. The stress of the dam heel should not appear as tensile stress; the actual compressive stress of the dam toe should not exceed the bearing capacity of concrete. Two mathematical equations for determining the stress based on the moment equilibrium of a rigid body can be used to define the limit-state functions of the two failure modes as follows:

$$Z_2 = P_{\min} \quad (3)$$

$$Z_3 = f_0 - P_{\max} \quad (4)$$

where P_{\min} is the stress of dam heel; P_{\max} is the stress of dam toe; and f_0 is the bearing capacity of concrete.

When using the finite element method to calculate P_{\min} and P_{\max} , the calculated results cannot be used as a basis for dam design and safety verification because of the stress concentration phenomenon. Fan et al. [26] proposed an equivalent stress method, which converts the stress obtained by the finite element method into the cross-sectional internal force, and uses the formula of material mechanics method to calculate the stress of the dam heel and toe, and the results obtained can be evaluated according to the design specification.

2.2. IPSO-LSSVM Model

2.2.1. LSSVM Principle

Suykens and Vandewalle initially proposed the LSSVM [27], which is an improvement of SVM. LSSVM uses fewer hyper-parameters than SVM. The quadratic programming issue

is converted into a linear system of equations using LSSVM, which substitutes equality constraints for inequality constraints in optimization problems. Reduced computational complexity, accelerated convergence, and improved solution correctness are all benefits of LSSVM. The principle of LSSVM is as follows:

Given a dataset $\{(x_i, y_i), i = 1, \dots, l\}$, $x_i \in R^d$ is a d -dimensional input vector and $y_i \in R$ is a scalar output. A regression function can be used to represent the nonlinear relationship between the input and output as:

$$f(x) = \omega^T \varphi(x) + b \tag{5}$$

where ω is the weight vector; $\varphi(x)$ is a nonlinear mapping from input space to high-dimensional feature space; and b is the deviation. The purpose of quadratic optimization in LSSVM is based on the structural risk reduction concept and is as follows:

$$\begin{aligned} \min & \frac{1}{2} \|\omega\|^2 + \frac{1}{2} \gamma \sum_{i=1}^l e_i^2 \\ \text{s.t. } & \omega^T \varphi(x_i) + b + e_i = y_i, i = 1, \dots, l \end{aligned} \tag{6}$$

where e_i is the error variable and γ is the regularization parameter. The Lagrange multiplier $\lambda \in R^{l \times 1}$ is used to convert constrained optimization into unconstrained optimization to resolve the optimization problem.

$$\min J = \frac{1}{2} \|\omega\|^2 + \frac{1}{2} \gamma \sum_{i=1}^l e_i^2 - \sum_{i=1}^l \lambda_i (\omega^T \varphi(x_i) + b + e_i - y_i) \tag{7}$$

The Karush–Kuhn–Tucker (KKT) conditions for optimality are given by:

$$\begin{cases} \frac{\partial J}{\partial \omega} = 0 \rightarrow \sum_{i=1}^l \lambda_i \varphi(x_i) = \omega \\ \frac{\partial J}{\partial b} = 0 \rightarrow \sum_{i=1}^l \lambda_i = 0 \\ \frac{\partial J}{\partial e_i} = 0 \rightarrow \lambda_i = \gamma e_i, i = 1, 2, \dots, l \\ \frac{\partial J}{\partial \lambda_i} = 0 \rightarrow \omega^T \varphi(x_i) + b + e_i - y_i = 0, i = 1, 2, \dots, l \end{cases} \tag{8}$$

After eliminating e_i and ω , the following linear equation set is obtained:

$$\begin{bmatrix} 0 & Q_l^T \\ Q_l & K + \gamma^{-1}I \end{bmatrix} \begin{bmatrix} b \\ A \end{bmatrix} = \begin{bmatrix} 0 \\ Y \end{bmatrix} \tag{9}$$

where $Q_l = [1, 1, \dots, 1]^T$ is an l -dimensional column vector; I is the identity matrix; $Y = [y_1, y_2, \dots, y_m]^T$ is the output vector of the training set; $A = [\lambda_1, \lambda_2, \dots, \lambda_m]^T$; K is the kernel function, $K(x_i, x_j) = \varphi(x_i)^T \varphi(x_j)$.

The dot product operation in the high-dimensional feature space is replaced by using K to transfer the original input space to the high-dimensional space. The regression function can be expressed as:

$$y = \sum_{i=1}^l \lambda_i K(x_i, x_j) + b \tag{10}$$

2.2.2. PSO Algorithm Principle

Iterative optimization is the basis of the evolutionary computation algorithm known as PSO optimization [28]. The PSO algorithm creates massless particles to represent the birds in the swarm. The particle has two attributes: position and velocity. The position represents the direction of movement, and the velocity represents the speed of movement. To identify

the optimal fitness as the present global optimum, each particle independently finds the optimal solution in the search space, records it as the fitness of the current individual, and shares the fitness with other particles in the complete particle swarm. Then, all particles update their velocity and position according to the current individual fitness value and the current global optimum. The following equations are used to update the particle's position and velocity:

$$V_{id} = \tau V_{id} + C_1 r_1 (0,1)(P_{id} - X_{id}) + C_2 r_2 (P_{gd} - X_{id}) \tag{11}$$

$$X_{id} = X_{id} + V_{id} \tag{12}$$

where τ is the inertia weight coefficient; V_{id} and X_{id} represent the velocity and position of particle i in d dimension, respectively; r_1 and r_2 are a random number between 0 and 1, respectively; C_1 and C_2 are the learning constants; P_{id} represents the historical optimal solution of particle i in d dimension; and P_{gd} represents the optimal position of the whole swarm in d dimension.

2.2.3. IPSO Algorithm Principle

The particle searches iteratively with a quick convergence velocity for the global optimum at the beginning of the PSO algorithm. However, the velocity of convergence will decrease gradually with the iterative process. If the particle meets a local optimum, all particles' velocities will eventually reach zero, and the swarm's evolution will come to an end.

To address the issue of the local optimum of the PSO algorithm being easily trapped, an improved particle swarm optimization (IPSO) algorithm is proposed to avoid falling into the local optimum. Improvements were achieved in the following three aspects:

(1) Generation of the initial swarm

The generation of the initial swarm is random. The likelihood of obtaining the global optimum is usually small since the particles are always not evenly dispersed in space. If too many particles are used, the optimization time and cost will be increased. Therefore, the swarm will almost certainly enter the local optimum if the limited number of particles cannot be dispersed over space. The average particle distance is defined as follows:

$$D(t) = \frac{1}{mH} \sum_{i=1}^m \sqrt{\sum_{d=1}^n (P_{id} - \bar{P}_d)^2} \tag{13}$$

where H is the length of the search space's longest diagonal; n is the search space's dimensionality; \bar{P}_d is the average of all particle locations' coordinates in the d -th dimension; and m is the number of particles in the swarm.

The average particle distance reflects the aggregation degree of distribution among particles. The smaller the $D(t)$, the denser the swarm.

(2) Determination of premature convergence

The overall fitness change in all particles can be used to identify the state of the swarm because a particle's position affects its fitness. If \bar{f} is the current average fitness of the swarm and f_i is the present fitness of particle i , then the following definition can be used to describe the fitness variance of the swarm:

$$\psi^2 = \sum_{i=1}^m \left(\frac{f_i - \bar{f}}{f} \right)^2 \tag{14}$$

where f is a normalized scaling factor. The value formula is:

$$f = \begin{cases} \max |f_i - \bar{f}|, & \max |f_i - \bar{f}| > 1 \\ 1, & \text{other} \end{cases} \tag{15}$$

Fitness variance reflects the degree of particle aggregation. The smaller the ψ^2 , the denser the swarm. The fitness of all particles tends to be consistent with the iterative process, so the ψ^2 becomes smaller and smaller. If ψ^2 is lower than a certain threshold, we can consider that the PSO algorithm enters the post-search phase. The swarm will easily become stuck in local optimum solutions at this time, leading to premature convergence.

(3) Improvement of inertia weight coefficient and learning constants

τ reflects the degree to retain the last iteration velocity. During the early search period, a large value is beneficial to the global searching ability. During the later search period, the low value is beneficial to the local searching ability. To balance the global searching ability and local searching ability, an inertia weight coefficient decreasing in parabolic form was proposed:

$$\tau = (\tau_{\max} - \tau_{\min}) \left(\frac{k}{k_{\max}} \right)^2 + (\tau_{\min} - \tau_{\max}) \left(2 \frac{k}{k_{\max}} \right) + \tau_{\max} \tag{16}$$

where τ_{\max} and τ_{\min} represent the maximum value and the min value of inertia weight coefficient, respectively. The τ_{\max} and τ_{\min} are generally accepted as: $\tau_{\max} = 0.9$ and $\tau_{\min} = 0.4$ [29]; k is the number of iterations; and k_{\max} is the maximum number of iterations.

C_1 represents the particle’s judgment of the best moving direction and represents the particle’s judgment affected by other particles. During the early search period, the value of C_1 should be large and the value of C_2 should be small to enhance the particle’s global search ability. During the later search period, the value of C_1 should be small and the value of C_2 should be large to make particles find the global optimum quickly. Therefore, the dynamic adjustment strategy of learning constants is introduced:

$$\begin{cases} C_1 = (C_{\min} - C_{\max}) \frac{k}{k_{\max}} + C_{\max} \\ C_2 = (C_{\max} - C_{\min}) \frac{k}{k_{\max}} + C_{\min} \end{cases} \tag{17}$$

The basic idea of the IPSO algorithm is as follows: Under the condition of ensuring the uniform distribution of the initial swarm, the PSO algorithm is first used in the optimization process until the particles are judged to fall into the premature state, and then the particles are redistributed in the solution space to help the particles to jump out of the local optimum quickly and accelerate the convergence.

The pseudo-code of the IPSO algorithm is detailed in Algorithm 1.

Algorithm 1: Pseudo-code of the IPSO algorithm

- 1: Define $m, \tau_{\max}, \tau_{\min}, C_{\max}, C_{\min}, k_{\max}$
 - 2: Define the boundaries of the optimization problem
 - 3: Initialize particle swarm
 - 4: Compute f, \bar{f} , and \bar{P}_d ; record P_{id} and P_{gd}
 - 5: for $k = 1$ to k_{\max} do
 - 6: Compute $D(t)$ and σ^2 of swarm using Equations (13) and (14)
 - 7: if $D(t) < \alpha$ and $\psi^2 < \delta$ then
 - 8: Initialize particle swarm
 - 9: re-record P_{id} and P_{gd}
 - 10: end
 - 11: for $i = 1$ to m do
 - 12: Compute each particle’s velocity using Equation (11)
 - 13: Update each particle’s position using Equation (12)
 - 14: end
 - 15: Update P_{id} and P_{gd}
 - 16: Compute f, \bar{f} , and \bar{P}_d
 - 17: end
-

2.2.4. Establishment of the IPSO-LSSVM Model

In this paper, the radial basis kernel function was selected as the kernel function of LSSVM. Therefore, the regularization parameter γ and the kernel width parameter σ are two important hyper-parameters of the LSSVM model. γ controls model complexity and penalties for exceeding errors. σ affects the training and prediction speed of the model. The IPSO algorithm was used for hyper-parameters tuning of the LSSVM model, and the IPSO-LSSVM model was established.

The steps were as follows:

- Step 1: Divide dataset into training set and testing set in a certain proportion.
- Step 2: Normalize the data of the training set and testing set.
- Step 3: Set the parameters of the IPSO algorithm.
- Step 4: Tune the γ and σ using the IPSO algorithm.
- Step 5: Input the hyper-parameters into the LSSVM model and establish the IPSO-LSSVM model.
- Step 6: Evaluate the accuracy of the IPSO-LSSVM model.

2.3. Method for Calculating the Reliability of Concrete Gravity Dams

The IPSO-LSSVM model combined with the MC method was used to calculate the reliability of concrete gravity dams. The analysis steps were as follows:

- (1) The main failure modes were determined and the influencing factors were selected. The statistical characteristic and value ranges of the factors were determined for a typical dam. In this paper, three failure modes of the dam were considered, which are sliding instability along the dam–ground surface and the overstress of dam heel and dam toe. The limit-state functions of the three failure modes are Equations (1), (3), and (4), respectively.
- (2) Taking reasonable assumptions, an appropriate finite element model was established. The foundation calculation range of the finite element model was reasonably selected.
- (3) Latin hypercube sampling was used to generate a certain number of samples to form a sample set. Taking K_c , P_{\min} , and P_{\max} as safety indexes, a finite element calculation batch program of concrete gravity dams was written using Python to calculate each sample to obtain the safety indexes.
- (4) A total of 80% of the samples were used as the training set and 20% of the samples were used as the testing set. The IPSO-LSSVM model was established to replace the finite element calculation.
- (5) Based on the IPSO-LSSVM model, the limit state functions of the three failure modes of the concrete gravity dam were constructed. The P_f was calculated by the MC method.

The flow chart is shown in Figure 1.

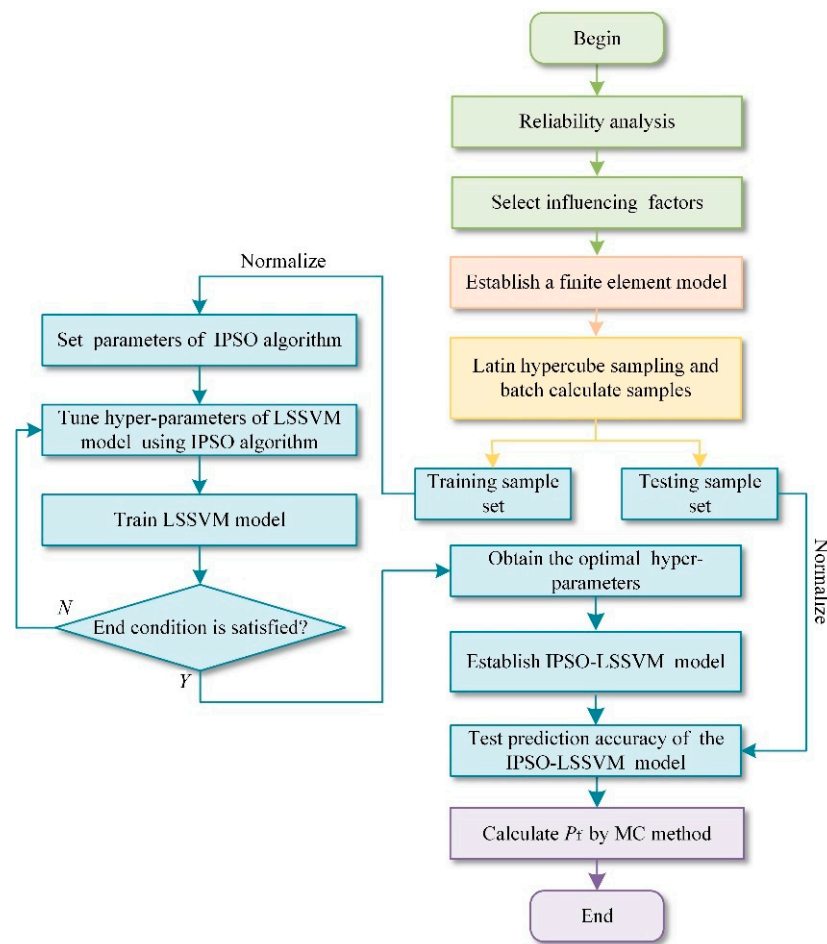


Figure 1. Flow chart of calculating the reliability of concrete gravity dams.

3. Case Study and Results

3.1. Basic Information of a Typical Concrete Gravity Dam

A typical gravity dam located in Yunnan Province of China was selected. The gravity dam is a roller-compacted concrete gravity dam. The dam is 106.00 m high, 17.50 m wide at the top, and 90.10 m wide at the base. The normal storage level is 1472.00 m, with a corresponding downstream water level of 1408.20 m. The designed flood level is 1478.35 m, with a corresponding downstream water level of 1423.46 m. The check flood level is 1480.26 m, with a corresponding downstream water level of 1425.23 m and an upstream dead water level of 1429.00 m. The foundation of this project is mainly hard slate with an elevation of 1375.00 m. A non-overflow dam section was selected for analysis. The profile of the section is shown in Figure 2. The statistical characteristics and value ranges of the influencing factors considered are shown in Table 1.

Table 1. Statistical characteristic and value ranges of the considered factors.

Factor	Type of Probability Distribution	Mean	Standard Deviation	Value Range
Upstream water level (m)	Truncated Normal Distribution	102.00	5.10	97.00–105.26
Downstream water level (m)	Truncated Normal Distribution	43.20	2.59	33.20–50.23
Concrete elasticity modulus (GPa)	Truncated Normal Distribution	28.0	2.8	25.2–30.8
Foundation elasticity modulus (GPa)	Truncated Normal Distribution	26.0	2.6	23.4–28.6
Anti-shear friction coefficient	Truncated Normal Distribution	1.00	0.22	0.90–1.10
Anti-shear cohesion (kPa)	Truncated Normal Distribution	900	360	700–1100
Concrete compressive strength (MPa)	Truncated Normal Distribution	11.20	2.24	6.80–13.00

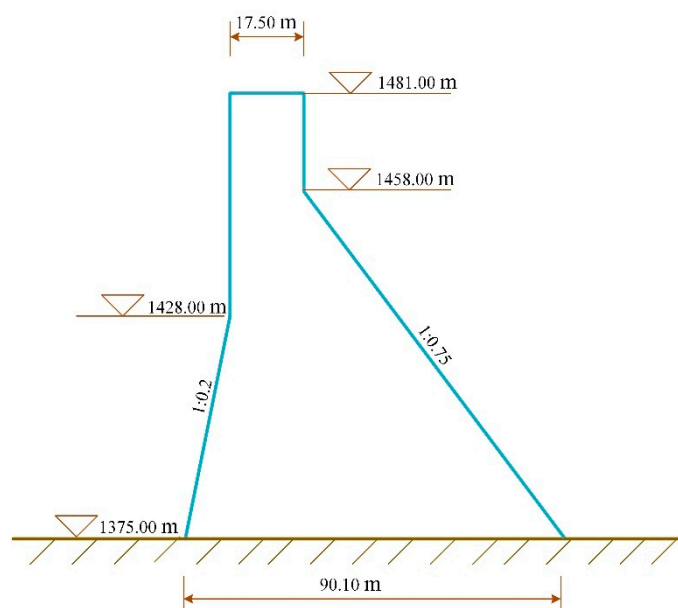


Figure 2. Typical profile of a gravity dam.

3.2. Finite Element Model of a Typical Concrete Gravity Dam

According to the basic information, a two-dimensional plane strain finite element model of the typical concrete gravity dam was established. The foundation rock is homogeneous characterized by the Mohr–Coulomb model [30]. The linear elastic model was adopted in dam concrete which is in good condition. A thin layer with a height of 0.2 m was used to simulate the contact between the dam and the foundation [30], and its material properties were consistent with foundation rock. Foundation boundary conditions were set to apply fixed constraints at the bottom of the foundation and horizontal constraints at the upstream and downstream of the foundation. The foundation and the dam were considered to be impervious. Dam weight and hydrostatic pressure acting on the upstream and downstream surfaces of the dam body and the foundation were taken into account. The main material properties of dam concrete, foundation rock, and contact are shown in Table 2.

Table 2. Main material properties. Calculation results.

Material	Elasticity Modulus (GPa)	Density (kg/m ³)	Poisson Ratio	Friction Angle (°)	Cohesion (MPa)
Dam concrete	28	2400	0.17	-	-
Foundation rock	26	2600	0.25	35	15
Contact	26	2600	0.25	35	15

When the finite element method is used to calculate the dam stress, the calculation domain needs to include the dam foundation. To reflect the influence of foundation stiffness on dam stress, the foundation was selected to a certain range, but in fact, the foundation was a semi-infinite space. To simplify the infinite space with limited space, the general way is to simulate by applying boundary constraints. According to the Saint-Venant principle, if the range of foundation considered is larger, the influence of boundary constraints on dam stress is smaller. When it reaches a certain range, the dam stress is almost no longer affected by the expansion of the foundation range. However, scholars do not have the same standard for the selection of foundation range.

In this section, the foundation range of the finite element model for the stress of the dam toe and heel and anti-sliding stability analysis was selected by calculation. The calculation diagram of foundation range selection is shown in Figure 3, in which $a = 0, 1, \dots, 9$ and $1 h$ is equal to 1 times the height of the dam.

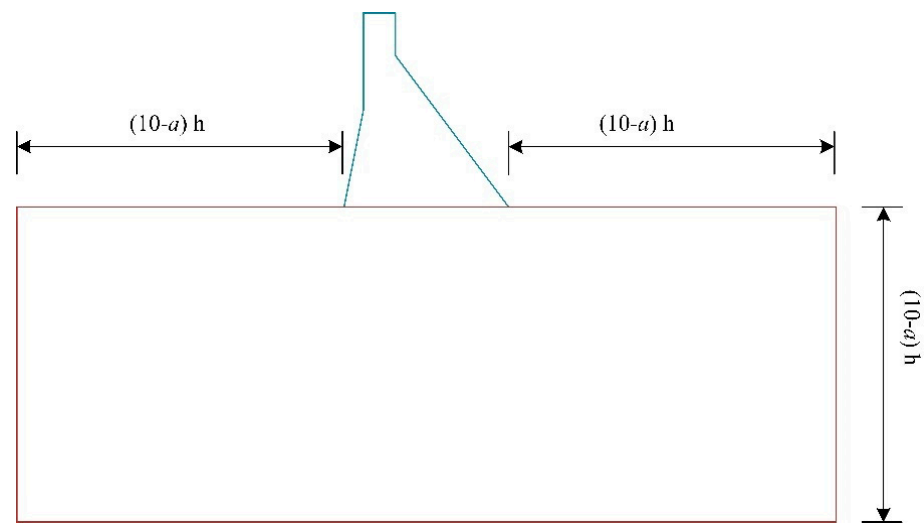


Figure 3. The calculation diagram of the foundation range selection.

With a increases from 0 to 9, in turn, the influence of the foundation range change on the calculation results of K_c , P_{max} , and P_{min} was analyzed. The results are shown in Table 3 and Figure 4.

Table 3. Calculation results.

Foundation Range (h)	K_c	P_{max} (MPa)	P_{min} (MPa)
1	5.05009	1.66877	1.15384
2	5.05526	1.66830	1.15835
3	5.05232	1.66856	1.15559
4	5.05157	1.66869	1.15505
5	5.05145	1.66864	1.15499
6	5.05095	1.66869	1.15457
7	5.05058	1.66872	1.15426
8	5.05030	1.66875	1.15403
9	5.05009	1.66877	1.15384
10	5.05008	1.66878	1.15383

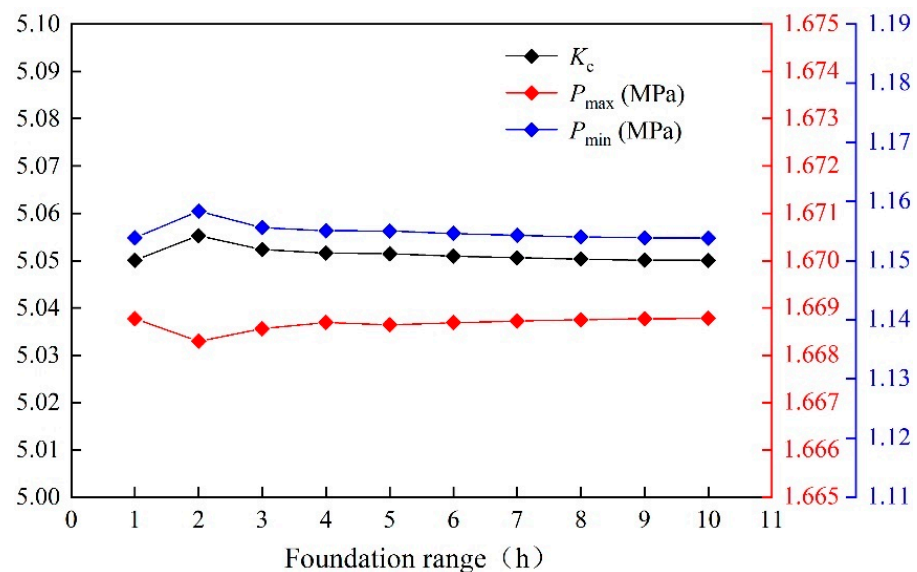


Figure 4. The influence of the foundation range change on the calculation results.

The results show that the values of K_c and P_{\min} first increase and then decrease with the increase in the foundation range. The influence of the foundation range on K_c and P_{\min} is small. With the foundation range increasing from 1 h to 10 h, the values of K_c and P_{\min} change to 0.00518 and 480 Pa, respectively. The values tend to become stable after the foundation range is greater than 3 h. The value of P_{\max} first decreases and then increases with the increase in the foundation range. The influence of the foundation range on the P_{\max} is also small. After the foundation range is greater than 3 h, the value tends to be stable. Therefore, in the finite element model, the foundation range is as follows: the length of the upstream foundation, length of the downstream foundation, and depth of the foundation were taken as 3 h.

3.3. Process of Establishing the IPSO-LSSVM Model

3.3.1. Selection of the Hyper-Parameters of LSSVM Model

σ and γ have a significant impact on the accuracy of the LSSVM model. In the following steps, the σ and γ of the model are tuned by the IPSO algorithm.

(1) Generation of sample sets

Latin hypercube sampling was used to generate 100 sets of samples. The K_c , P_{\min} , and P_{\max} of each set of samples were obtained by the finite element model of the gravity dam. A total of 80% of these samples were used to train the IPSO-LSSVM model, and the other 20% of these samples were used to test the accuracy of the model. To facilitate the calculation, a finite element calculation batch program of concrete gravity dams was written using Python to automatically calculate and extract the results of each sample by calling Abaqus. The steps were as follows:

1. Use Python language to generate inp files for each sample in bulk.
 2. Use Python language to generate bat files to submit calculations in bulk.
 3. Use Python language to extract numerical simulation results from all odb files.
- ##### (2) Data pre-processing

To make different datasets comparable, it was necessary to normalize all data.

$$x_n = \frac{x - x_{\min}}{x_{\max} - x_{\min}} \quad (18)$$

where x_{\max} and x_{\min} are the maximum and minimum value of variable x , respectively, and x_n is normalized data.

(3) Setting of the IPSO algorithm parameters

The IPSO algorithm was used for hyper-parameters tuning of the LSSVM. We set the IPSO algorithm parameters as: $m = 20$, $k_{\max} = 40$, $\tau \in [0.4, 0.9]$, $C_{\max} = 2.5$, $C_{\min} = 0.5$, $\sigma \in [0.0001, 4000]$, and $\gamma \in [0.0001, 3000]$, and the function fitness was the mean relative error (MRE).

(4) Optimization results

From Figures 5–7, it can be seen that, in the process of the IPSO algorithm to tune the hyper-parameters of the three models, the global optimal fitness curve appears to suddenly bulge. The PSO algorithm appears to be the aggregate phenomenon in the process of optimization, which will lead to falling into the local optimum. The IPSO algorithm introduces the fitness variance of the swarm to control the degree of particle aggregation. When the swarm is too aggregated, the particles will be re-dispersed for optimization. Therefore, this phenomenon occurs. This proves that the IPSO algorithm can overcome the shortcomings of the PSO algorithm as the initial convergence can easily fall into the local optimum.

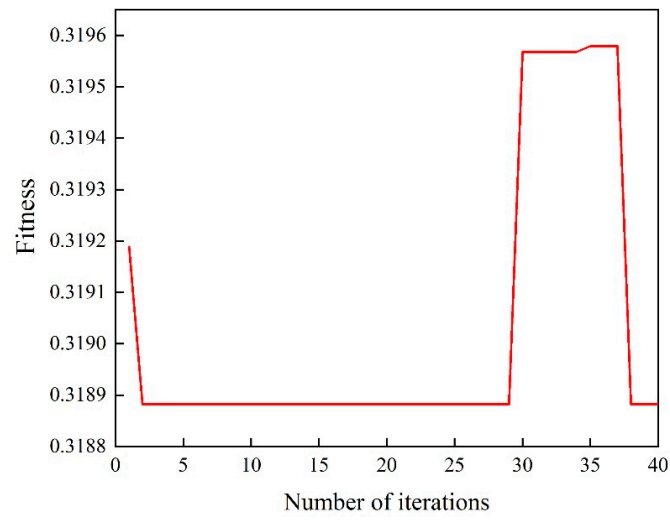


Figure 5. Optimization curve of the function fitness of the model of K_c .

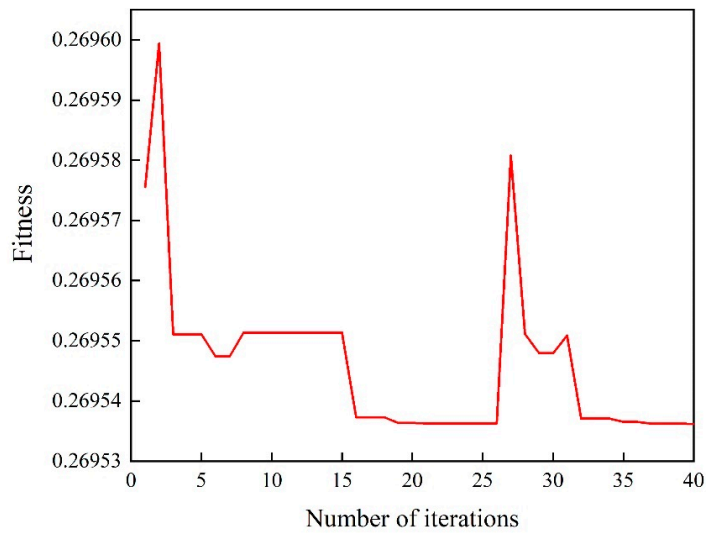


Figure 6. Optimization curve of the function fitness of the model of P_{min} .

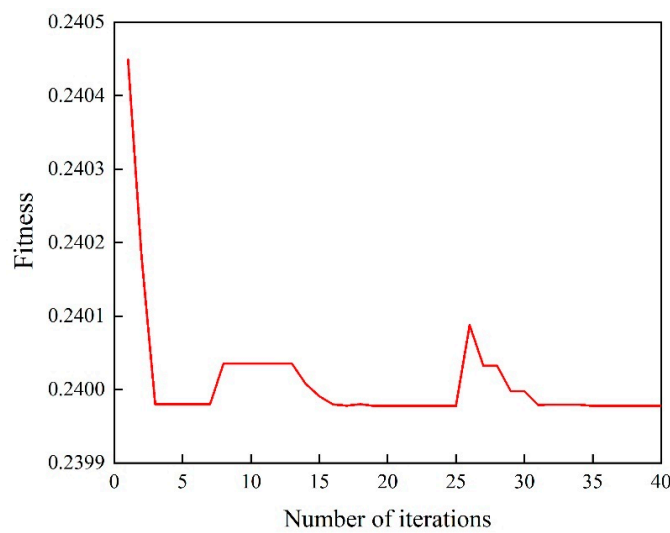


Figure 7. Optimization curve of the function fitness of the model of P_{max} .

Table 4 shows the optimal γ and σ of the three models, and inputs the optimal hyper-parameters into the LSSVM models to establish the IPSO-LSSVM models.

Table 4. Optimization results.

Optimization Algorithm	K_c		P_{\min}		P_{\max}	
	σ	γ	σ	γ	σ	γ
IPSO	1928	2823	1833	2996	1771	2653

3.3.2. Comparison of the Accuracy of the Models

The coefficient of determination (R^2), the mean absolute error (MAE), and the root-mean-square error ($RMSE$) were adopted as the evaluation indexes of model accuracy. The accuracy of the IPSO-LSSVM models of K_c , P_{\min} , and P_{\max} were compared with that of RSM and PSO-LSSVM models. The comparison results are shown in Table 5. The comparison between the predicted value and true value of K_c , P_{\min} , and P_{\max} is shown in Figures 8–10.

Table 5. The comparison results of the accuracy.

K_c			
Model	R^2	MAE	$RMSE$
RSM	0.7194	0.1261	0.2230
PSO-LSSVM	0.8638	0.0486	0.0762
IPSO-LSSVM	0.9762	0.0214	0.0239
P_{\min}			
Model	R^2	MAE	$RMSE$
RSM	0.6019	0.0256	0.0427
PSO-LSSVM	0.8319	0.0051	0.0085
IPSO-LSSVM	0.9803	0.0016	0.0021
P_{\max}			
Model	R^2	MAE	$RMSE$
RSM	0.6053	0.0282	0.0474
PSO-LSSVM	0.8726	0.0050	0.0078
IPSO-LSSVM	0.9904	0.0015	0.0018

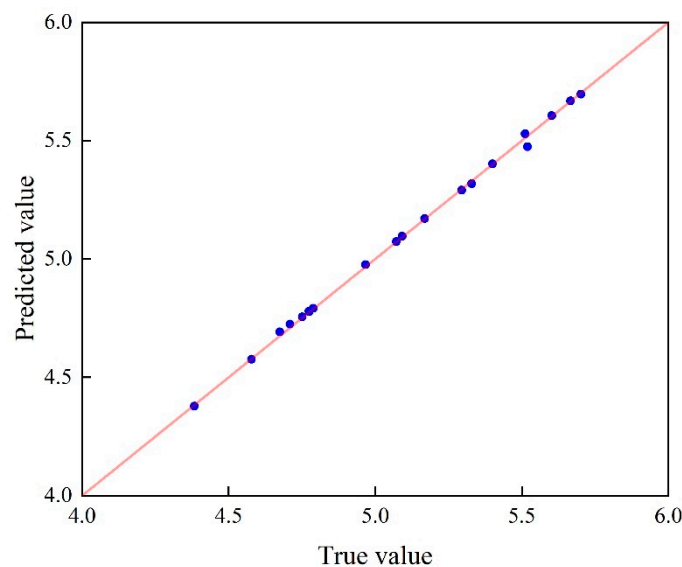


Figure 8. Comparison between the predicted and true value of K_c .

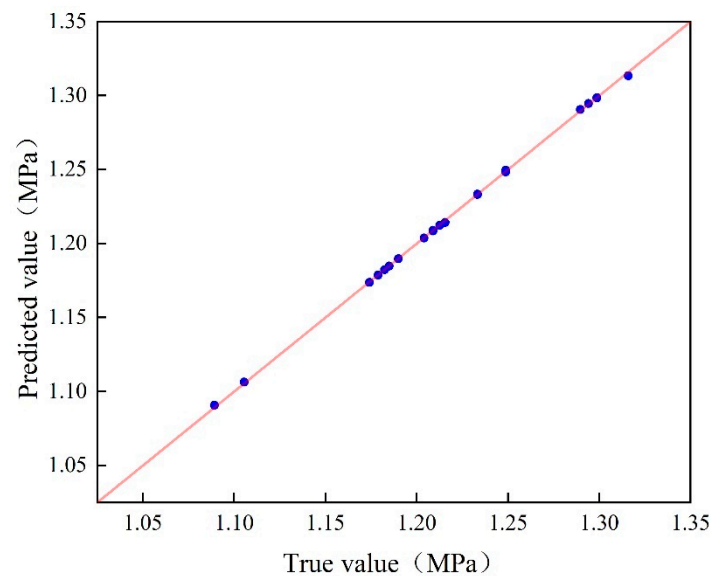


Figure 9. Comparison between the predicted and true value of P_{\min} .

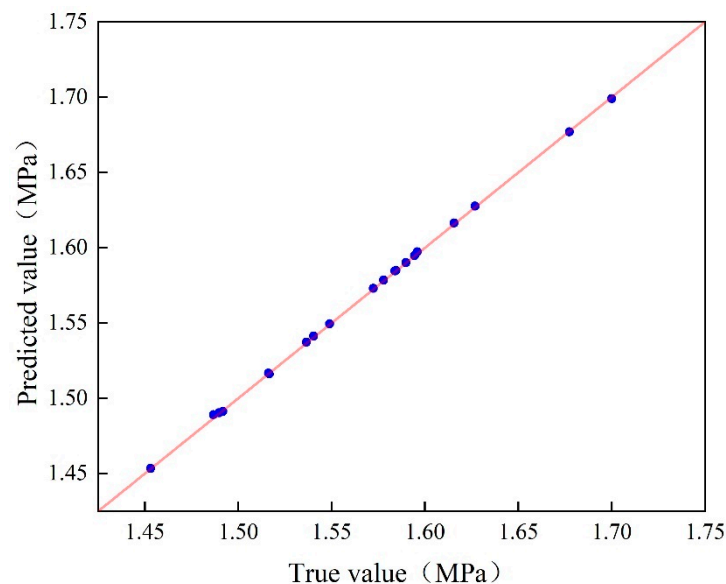


Figure 10. Comparison between the predicted and true value of P_{\max} .

It can be seen from Table 5 that the accuracy of the RSM models is the lowest, indicating a highly nonlinear relationship between the influencing factors and the safety indexes of the concrete gravity dam. The accuracy of the remaining two models is higher, among which the IPSO-LSSVM models have the highest accuracy. The accuracy of the IPSO-LSSVM models is significantly improved compared with that of the PSO-LSSVM models, indicating that the IPSO algorithm is better at tuning the hyper-parameters of the LSSVM model than the PSO algorithm. Therefore, the IPSO-LSSVM model has significant advantages for dealing with highly nonlinear problems, and the IPSO algorithm is outstanding for the optimal solution of complex problems.

Figures 8–10 show that the linear relationship between the predicted and true value is $y = x$, indicating that the IPSO-LSSVM models are reliable, which can be used for the reliability calculation of concrete gravity dams.

3.4. Reliability Calculation

Based on the IPSO-LSSVM model, the limit state functions (Equations (1), (3), and (4)) of the three failure modes of the concrete gravity dam were constructed. The MC method

was used to calculate the P_f of the typical concrete gravity dam. The MC method requires a sufficiently large sample to achieve high accuracy, and the quality of the calculated results is generally evaluated using the coefficient of variation of P_f . When the coefficient of variation of P_f is less than 0.1, the results are considered to meet the accuracy requirements [31]. Under the most unfavorable conditions, the K_c and P_{min} of the concrete gravity dam meet the safety requirements, so this section mainly analyzes the probability of stress exceedance at the toe of the dam. The probability of stress exceedance at the toe of the dam was calculated 10 times for different sample sizes to obtain the mean value and the coefficient of variation of P_f . The results are shown in Table 6, and the curve of P_f is shown in Figure 11.

Table 6. Calculation results of the probability of stress exceedance at the toe of the dam.

Number of Samples	P_f	Coefficient of Variation
1	0	-
10	0	-
10^2	0	-
10^3	0	-
10^4	9.00×10^{-5}	1.05
10^5	7.45×10^{-5}	0.44
10^6	8.87×10^{-5}	0.07

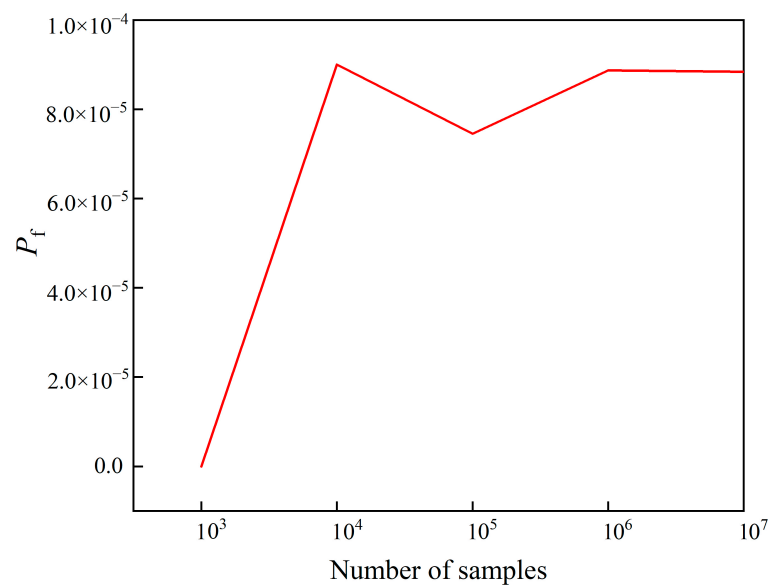


Figure 11. The curve of P_f .

From the results, it can be seen that, when the number of samples exceeds 10^6 , the coefficient of variation of P_f is already less than 0.1, indicating the results meet the accuracy requirements. The P_f calculated by using the IPSO-LSSVM model is stable at 8.87×10^{-5} . Since there is only one failure mode, the P_f of the concrete gravity dam system is 8.87×10^{-5} , which is much smaller than the value specified in the specification, so the concrete gravity dam is safe and reliable.

4. Discussion

In many cases, due to the complexity of reliability analysis problems, it is hard to establish an effective response surface to assess the P_f of concrete gravity dams. A reliability analysis method based on the IPSO-LSSVM was proposed to calculate the reliability of concrete gravity dams when explicit nonlinear limit-state functions are difficult to obtain accurately. In the method, the hyper-parameters of the LSSVM model were tuned by the IPSO algorithm to reflect the relationship between the influencing factors and safety

indexes. After that, the IPSO-LSSVM model was utilized in conjunction with the MC method to evaluate the failure probability.

Accurate expression of limit state function is the key to obtain reliable calculation results. This paper focused on the improvement method for the accuracy of the model used for reliability analysis of concrete dams. The RSM models were used to test the degree of nonlinearity between the influencing factors and safety indexes and the results show a highly nonlinear relationship between the influencing factors and the safety indexes. The accuracy of the IPSO-LSSVM model was compared with that of the PSO-LSSVM model, and the result shows that the IPSO-LSSVM has higher accuracy, indicating that the IPSO-LSSVM model significantly improves the accuracy of the PSO-LSSVM model.

In the case study, the number of samples required for P_f calculation is 10^6 . If the traditional Monte Carlo-finite element method is used to calculate P_f , then it consumes more than 2000 h. However, the method proposed in this paper can effectively shorten computing time; it only takes about 20 min, so its computing efficiency is greatly improved. Therefore, the method proposed in this paper can effectively improve computing efficiency on the precondition of accuracy maximization.

The main contribution of this paper is its improvement of the established model [32] and short computing time compared with the traditional reliability analysis method. The proposed reliability analysis method is shown to be an efficient scheme with respect to both computational effort and accuracy.

5. Conclusions

The main research results are summarized as follows:

- (1) The IPSO algorithm was proposed by introducing average particle distance, swarm fitness variance, inertia weight coefficient decreasing in parabolic form, and dynamic adjustment strategy of learning constants into the PSO algorithm. The hyper-parameters of the LSSVM model were tuned by the IPSO algorithm to establish IPSO-LSSVM model. The comparison results show that the IPSO-LSSVM model significantly improves the accuracy of the PSO-LSSVM model.
- (2) The case study indicates that the proposed reliability analysis method based on the IPSO-LSSVM can highly efficiently and accurately determine failure probability of concrete dams so that it is effective and feasible.
- (3) The reliability analysis method proposed in this paper can provide an effective tool for solving the reliability of other complex structures. The proposed method can also provide technical support for safety assessment, monitoring and operation management of gravity dams. In future studies, more complex engineering problems will be solved, such as considering the impact of environmental erosion and material aging on the dam safety. The proposed methods can play an important role in solving these problems together with other existing methods.

Author Contributions: Conceptualization, B.X.; methodology, B.X.; software, S.W.; validation, S.W.; investigation, S.W.; resources, S.W.; data curation, S.W.; writing—original draft preparation, S.W.; writing—review and editing, Z.Z.; visualization, J.L. (Jing Li) and J.L. (Junyi Lu); supervision, Z.Z.; project administration, Z.Z.; funding acquisition, B.X. All authors have read and agreed to the published version of the manuscript.

Funding: The present work was supported by the National Natural Science Foundation of China (Grant No. 52079120).

Institutional Review Board Statement: Not applicable.

Informed Consent Statement: Not applicable.

Data Availability Statement: The data that support the findings of this study are available from the corresponding author, B.X., upon reasonable request.

Conflicts of Interest: The authors declare no conflict of interest.

References

1. Pei, L.; Chen, C.; He, K.; Lu, X. System Reliability of a Gravity Dam-Foundation System Using Bayesian Networks. *Reliab. Eng. Syst. Saf.* **2022**, *218*, 108178. [\[CrossRef\]](#)
2. Sharafati, A.; Yaseen, Z.M.; Pezeshki, E. Strategic Assessment of Dam Overtopping Reliability Using a Stochastic Process Ap-proach. *J. Hydrol. Eng.* **2020**, *25*, 04020029. [\[CrossRef\]](#)
3. Yang, Z.; Ching, J. A Novel Reliability-Based Design Method Based on Quantile-Based First-Order Second-Moment. *Appl. Math. Modell.* **2020**, *88*, 461–473. [\[CrossRef\]](#)
4. Metropolis, N.; Ulam, S. The Monte Carlo Method. *J. Am. Stat. Assoc.* **1949**, *44*, 335–341. [\[CrossRef\]](#) [\[PubMed\]](#)
5. Fu, X.; Xie, S.; Li, J.; Zhu, C.; Zhang, X. Strain Response Based Finite Element Model Updating by Using Response Surface Method. *Int. J. Appl. Electromagn. Mech.* **2016**, *52*, 1087–1097. [\[CrossRef\]](#)
6. Nie, X.-B.; Li, H.-B. A Direct-Integration-Based Structural Reliability Analysis Method Using Non-Probabilistic Convex Model. *J. Mech. Sci. Technol.* **2018**, *32*, 5063–5068. [\[CrossRef\]](#)
7. Zhao, Y.-G.; Ang, A.H.-S. On the First-Order Third-Moment Reliability Method. *Struct. Infrastruct. Eng.* **2012**, *8*, 517–527. [\[CrossRef\]](#)
8. Lu, Z.-H.; Hu, D.-Z.; Zhao, Y.-G. Second-Order Fourth-Moment Method for Structural Reliability. *J. Eng. Mech.* **2017**, *143*, 06016010. [\[CrossRef\]](#)
9. Yeşiltaş, Ö.; Özcan, A. Spin and Pseudospin Symmetries in Radial Dirac Equation and Exceptional Hermite Polynomials. *Eur. Phys. J. Plus.* **2021**, *136*, 1035. [\[CrossRef\]](#)
10. Ren, Z.; Zhang, D.; Koh, C. Investigation of Reliability Analysis Algorithms for Effective Reliability-based Optimal Design of Electromagnetic Devices. *IET Sci. Meas. Technol.* **2016**, *10*, 44–49. [\[CrossRef\]](#)
11. Heydt, G.T.; Graf, T.J. Distribution System Reliability Evaluation Using Enhanced Samples in a Monte Carlo Approach. *IEEE Trans. Power Syst.* **2010**, *25*, 2006–2008. [\[CrossRef\]](#)
12. Engelund, S.; Rackwitz, R. A Benchmark Study on Importance Sampling Techniques in Structural Reliability. *Struct. Saf.* **1993**, *12*, 255–276. [\[CrossRef\]](#)
13. Guan, X.L.; Melchers, R.E. Effect of Response Surface Parameter Variation on Structural Reliability Estimates. *Struct. Saf.* **2001**, *23*, 429–444. [\[CrossRef\]](#)
14. Zhu, X.; Wang, X.; Li, X.; Liu, M.; Cheng, Z. A New Dam Reliability Analysis Considering Fluid Structure Interaction. *Rock Mech. Rock Eng.* **2018**, *51*, 2505–2516. [\[CrossRef\]](#)
15. Zhao, H. High Dimension Model Representation-Based Response Surface for Reliability Analysis of Tunnel. *Math. Probl. Eng.* **2018**, *2018*, 1–10. [\[CrossRef\]](#)
16. Balu, A.S.; Rao, B.N. Confidence Bounds on Design Variables Using High-Dimensional Model Representation-Based Inverse Reliability Analysis. *J. Struct. Eng.* **2013**, *139*, 985–996. [\[CrossRef\]](#)
17. Sundar, V.S.; Shields, M.D. Surrogate-Enhanced Stochastic Search Algorithms to Identify Implicitly Defined Functions for Reliability Analysis. *Struct. Saf.* **2016**, *62*, 1–11. [\[CrossRef\]](#)
18. Yuan, X.-X.; Pandey, M.D. Analysis of Approximations for Multinormal Integration in System Reliability Computation. *Struct. Saf.* **2006**, *28*, 361–377. [\[CrossRef\]](#)
19. Hariri-Ardebili, M.A.; Pourkamali-Anaraki, F. Support Vector Machine Based Reliability Analysis of Concrete Dams. *Soil Dyn. Earthquake Eng.* **2018**, *104*, 276–295. [\[CrossRef\]](#)
20. Assaad, R.; El-adaway, I.H. Evaluation and Prediction of the Hazard Potential Level of Dam Infrastructures Using Computational Artificial Intelligence Algorithms. *J. Manage. Eng.* **2020**, *36*, 04020051. [\[CrossRef\]](#)
21. Trelea, I.C. The Particle Swarm Optimization Algorithm: Convergence Analysis and Parameter Selection. *Inf. Process. Lett.* **2003**, *85*, 317–325. [\[CrossRef\]](#)
22. Chamkalani, A.; Zendejboudi, S.; Bahadori, A.; Kharrat, R.; Chamkalani, R.; James, L.; Chatzis, I. Integration of LSSVM Technique with PSO to Determine Asphaltene Deposition. *J. Pet. Sci. Eng.* **2014**, *124*, 243–253. [\[CrossRef\]](#)
23. Gholgheysari Gorjaei, R.; Songolzadeh, R.; Torkaman, M.; Safari, M.; Zargar, G. A Novel PSO-LSSVM Model for Predicting Liquid Rate of Two Phase Flow through Wellhead Chokes. *J. Nat. Gas Sci. Eng.* **2015**, *24*, 228–237. [\[CrossRef\]](#)
24. Song, Y.; Xie, X.; Wang, Y.; Yang, S.; Ma, W.; Wang, P. Energy Consumption Prediction Method Based on LSSVM-PSO Model for Autonomous Underwater Gliders. *Ocean Eng.* **2021**, *230*, 108982. [\[CrossRef\]](#)
25. Roushangar, K.; Sagheblian, S.M.; Mouaze, D. Predicting Characteristics of Dune Bedforms Using PSO-LSSVM. *Int. J. Sediment Res.* **2017**, *32*, 515–526. [\[CrossRef\]](#)
26. Fan, S.; Chen, J.; Guo, J. Application of Finite Element Equivalent Stress Method to Analyze the Strength of Gravity Dams. *J. Hydraul. Eng.* **2007**, *38*, 754–759. [\[CrossRef\]](#)
27. Suykens, J.A.K.; Vandewalle, J. Least Squares Support Vector Machine Classifiers. *Neural Processing Lett.* **1999**, *9*, 293–300. [\[CrossRef\]](#)
28. Kennedy, J.; Eberhart, R. Particle Swarm Optimization. In Proceedings of the ICNN'95—International Conference on Neural Networks, Perth, WA, Australia, 27 November–1 December 1995; Volume 4, pp. 1942–1948. [\[CrossRef\]](#)
29. Feng, Y.; Teng, G.-F.; Wang, A.-X.; Yao, Y.-M. Chaotic Inertia Weight in Particle Swarm Optimization. In Proceedings of the 2nd International Conference on Innovative Computing, Information and Control, Kumamoto, Japan, 5–7 September 2007; p. 475. [\[CrossRef\]](#)

30. Li, Z. Global Sensitivity Analysis of the Static Performance of Concrete Gravity Dam from the Viewpoint of Structural Health Monitoring. *Arch. Computat. Methods Eng.* **2021**, *28*, 1611–1646. [[CrossRef](#)]
31. Marelli, S.; Sudret, B. An Active-Learning Algorithm That Combines Sparse Polynomial Chaos Expansions and Bootstrap for Structural Reliability Analysis. *Struct. Saf.* **2018**, *75*, 67–74. [[CrossRef](#)]
32. Kang, F.; Li, J.; Li, J. System Reliability Analysis of Slopes Using Least Squares Support Vector Machines with Particle Swarm Optimization. *Neurocomputing* **2016**, *209*, 46–56. [[CrossRef](#)]